

Crystal Structure of Layered Li-Ni-Mn-O Compounds

Yasuhiro Fujii, Hiroshi Miura, Naoto Suzuki, Takayuki Shoji, and Noriaki Nakayama*

Tosoh Co., Ltd, 4560 Kaisei-cho, Syunan, Yamaguchi 746-8501, Japan

Fax: 81-834-63-9896, e-mail: ya_fujii@tosoh.co.jp

*Faculty of Engineering, Yamaguchi University, 2-16-1 Tokiwadai, Ube, 755-8611, Japan

Fax: 81-836-85-9601, e-mail: nakayamn@yamaguchi-u.ac.jp

The crystal structure, thermal stability and electrochemical property of $\text{LiNi}_{1/2}\text{Mn}_{1/2}\text{O}_2$ and $\text{Li}_{2/3}\text{Ni}_{1/3}\text{Mn}_{2/3}\text{O}_2$ with layered rock-salt type structures have been investigated. $\text{LiNi}_{1/2}\text{Mn}_{1/2}\text{O}_2$ was prepared by a co-precipitation of Ni-Mn mixed hydroxides and the subsequent solid state reaction with LiOH. $\text{Li}_{2/3}\text{Ni}_{1/3}\text{Mn}_{2/3}\text{O}_2$ was prepared by an ion exchange reaction of $\text{Na}_{2/3}\text{Ni}_{1/3}\text{Mn}_{2/3}\text{O}_2$. $\text{LiNi}_{1/2}\text{Mn}_{1/2}\text{O}_2$ adopts an O3-type stacking in which a $\sqrt{3} \times \sqrt{3}$ superlattice is formed due to the cationic ordering. $\text{Li}_{2/3}\text{Ni}_{1/3}\text{Mn}_{2/3}\text{O}_2$ adopts a T2-type stacking and form a $\sqrt{3} \times \sqrt{3}$ superlattice due to the cationic ordering. However, electron diffraction patterns of $\text{Li}_{2/3}\text{Ni}_{1/3}\text{Mn}_{2/3}\text{O}_2$ show additional superlattice spots indicating the vacancy ordering in the tetrahedral Li layers. The thermal stability and the electrochemical properties are discussed based on the structural properties.

1. Introduction

In recent years, Li-Ni-Mn-O compounds with layered rock-salt type structures have been proposed as possible alternatives to LiCoO_2 widely used in current Li-ion batteries. Above all, $\text{LiNi}_{1/2}\text{Mn}_{1/2}\text{O}_2$ is one of the most possible candidates [1]. This structure is called O3 since the alkali cation (Li^+) is located in octahedral sites and the unit cell consists of three MO_2 sheets (MO_2 = transition metals) [2]. A Li defect phase with an O2 based structure, $\text{Li}_{2/3}\text{Ni}_{1/3}\text{Mn}_{2/3}\text{O}_2$, is also reported [3]. Although the atomic arrangement of Ni and Mn atoms in these phases has been investigated in several studies, it is still controversial [4-6]. Also the microscopic structures, such as the stacking disorder, have not been well characterized.

We have synthesized these compounds and characterized by using powder X-ray diffraction, transmission electron microscopy (TEM), and electrochemical measurements. Particularly the microscopic structures of these compounds have been investigated comparatively by using the TEM both in the plane and along the stacking direction. Also the thermal stabilities of the structure have been compared.

2. Experimental

$\text{LiNi}_{1/2}\text{Mn}_{1/2}\text{O}_2$ was prepared by heating the mixtures of lithium hydroxide and nickel-manganese mixed hydroxide. $\text{Li}_{2/3}\text{Ni}_{1/3}\text{Mn}_{2/3}\text{O}_2$ was prepared from $\text{Na}_{2/3}\text{Ni}_{1/3}\text{Mn}_{2/3}\text{O}_2$ by ion exchanging sodium for lithium in molten LiNO_3 at 280 °C for 12h. The $\text{Na}_{2/3}\text{Ni}_{1/3}\text{Mn}_{2/3}\text{O}_2$ was prepared from Mn_2O_3 , $\text{Ni}(\text{OH})_2$, and Na_2CO_3 . Solid-state reaction was performed in air at 900 °C for 1week.

Samples were identified and characterized by powder X-ray diffraction method. For TEM observations, samples were dispersed in ethanol by applying the ultrasonic wave and were collected on a holly micro grid supported on a copper grid mesh. A field emission type TEM (JEOL JEM2010F) operated at 200kV was used for the

observations. The thermal behavior of samples was examined using a TG (TG6300, Seiko Instruments) in air up to 1000 °C at a rate of 10 °C min⁻¹.

Electrochemical properties were examined with CR2032 type coin cells. The cell was comprised of a cathode and lithium metal anode separated by a polypropylene separator and glass fiber mat. The cathode consisted of 25mg of Li-Ni-Mn-O powders and 12mg conducting binder pressed on a stainless screen. The electrolyte solution was 1M LiPF_6/EC and DMC. The EC and DMC were mixed in a 1:2 volume ratio. The cell was charged and discharged in the voltage range of 2.5-4.5V at a current density of 0.1mA cm⁻² at 23 °C.

3. Results and discussion

3.1 XRD study

Powder X-ray diffraction patterns of $\text{Li}_{2/3}\text{Ni}_{1/3}\text{Mn}_{2/3}\text{O}_2$ and $\text{LiNi}_{1/2}\text{Mn}_{1/2}\text{O}_2$ are shown in Fig. 1. They are characteristic of the layered rock-salt type structure. However, the layer stacking is somewhat different. The XRD pattern of $\text{LiNi}_{1/2}\text{Mn}_{1/2}\text{O}_2$ can be indexed by assuming O3 stacking with the space group symmetry of $R\bar{3}m$ (α - NaFeO_2 type structure). The lattice parameters in the hexagonal setting are $a=2.89 \text{ \AA}$ and $c=14.31 \text{ \AA}$. The Rietveld refinement based on the $R\bar{3}m$ space group indicates that the 10% of Li sites are occupied by Ni atoms [7]. The XRD pattern of $\text{Li}_{2/3}\text{Ni}_{1/3}\text{Mn}_{2/3}\text{O}_2$ can be indexed by assuming a orthorhombic cell with the space group symmetry of $Cmca$ [8], in which the layers are stacked in the T2 mode and the Ni and Mn atoms are ordered to form an in-plane $[\sqrt{3} \times \sqrt{3}]R30^\circ$ type superlattice. The lattice parameters are $a=8.579 \text{ \AA}$, $b=4.953 \text{ \AA}$ and $c=10.05 \text{ \AA}$. The diffraction peaks of this phase are rather broader than those of $\text{LiNi}_{1/2}\text{Mn}_{1/2}\text{O}_2$ except for the main 002 reflection, suggesting the stacking disorder. It is to be noted that Ni and Mn atoms are divalent and tetravalent, respectively, according to the literatures [3,4,9].

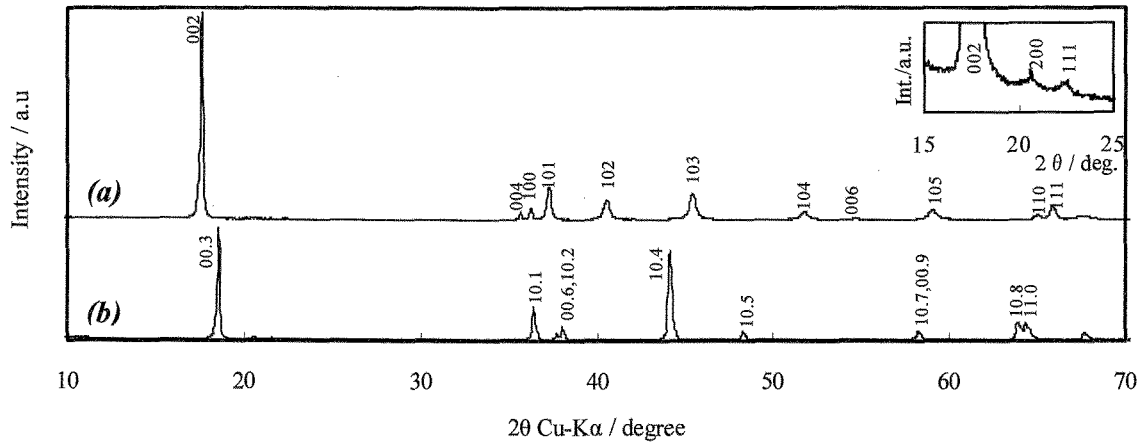


Figure 1. X-ray diffraction patterns of (a) $\text{Li}_{2/3}\text{Ni}_{1/3}\text{Mn}_{2/3}\text{O}_2$ and (b) $\text{LiNi}_{1/2}\text{Mn}_{1/2}\text{O}_2$. The inset shows an enlargement in the range $2\theta = 15\text{--}25^\circ$. The weak extra reflections in this range are indicative of the superlattice formation.

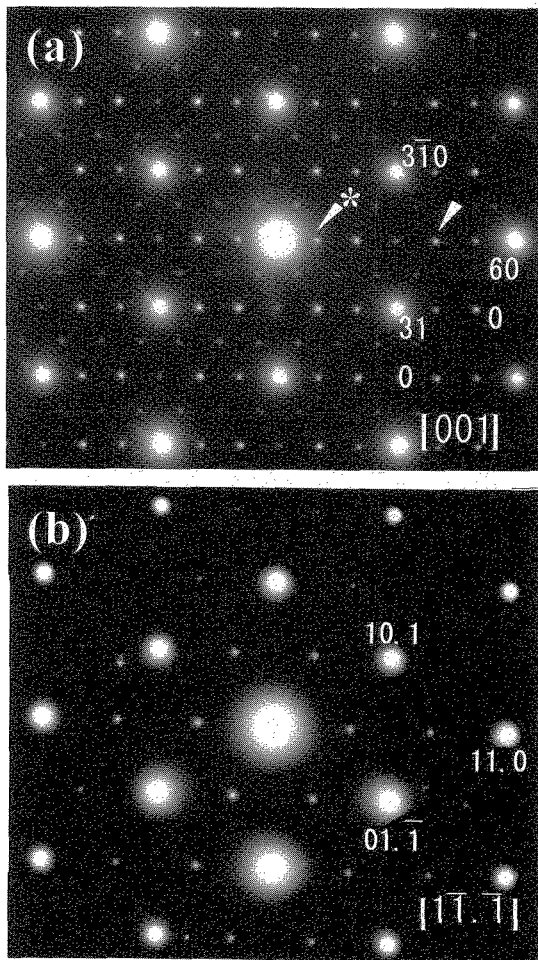


Figure 2. Electron diffraction patterns of (a) $\text{Li}_{2/3}\text{Ni}_{1/3}\text{Mn}_{2/3}\text{O}_2$ and (b) $\text{LiNi}_{1/2}\text{Mn}_{1/2}\text{O}_2$. The diffraction spots have been indexed assuming the orthorhombic Cmca structure for (a) and the $\text{R}\bar{3}\text{m}$ structure in hexagonal setting for (b). The extra spots due to the in plane $[\sqrt{3} \times \sqrt{3}]R30^\circ$ superlattice are marked by arrows. Those marked by asterisks suggest the vacancy ordering in the Li layer.

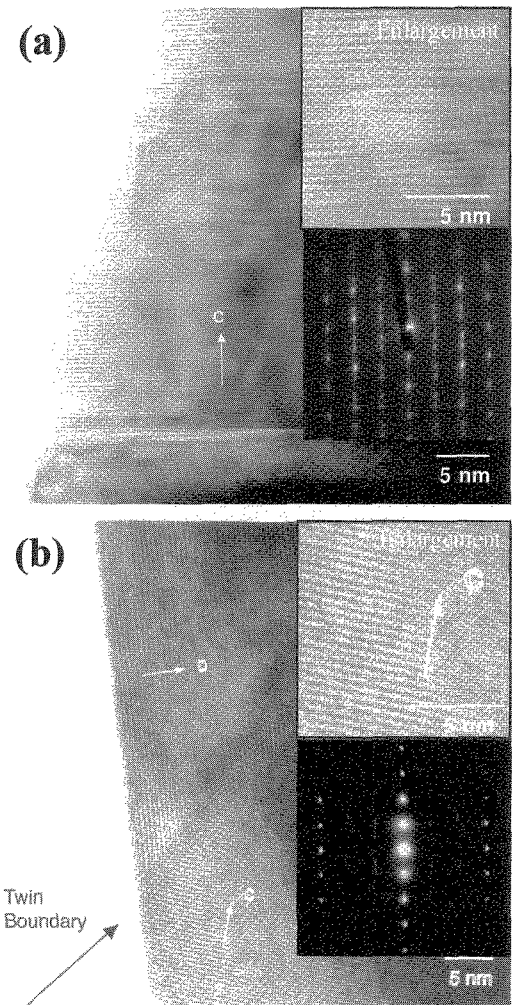


Figure 3. Lattice image of (a) $\text{Li}_{2/3}\text{Ni}_{1/3}\text{Mn}_{2/3}\text{O}_2$ and (b) $\text{LiNi}_{1/2}\text{Mn}_{1/2}\text{O}_2$ viewing along (a) $[110]$ and (b) $[11.0]$.

3.2 TEM study

Figures 2 (a) and (b) show an [001] zone electron diffraction pattern (EDP) of orthorhombic $\text{Li}_{2/3}\text{Ni}_{1/3}\text{Mn}_{2/3}\text{O}_2$ and a $[\bar{1}\bar{1}\bar{1}]$ zone EDP of rhombo-hexagonal $\text{LiNi}_{1/2}\text{Mn}_{1/2}\text{O}_2$, respectively. Both EDPs show extra spots, as marked by arrows in the figures, indicating a $[\sqrt{3} \times \sqrt{3}]R30^\circ$ superlattice in the basal plane [10]. Extra spots in the EDP of $\text{Li}_{2/3}\text{Ni}_{1/3}\text{Mn}_{2/3}\text{O}_2$ are more intense than those of $\text{LiNi}_{1/2}\text{Mn}_{1/2}\text{O}_2$. The regular $[\sqrt{3} \times \sqrt{3}]R30^\circ$ superlattice corresponds to the 1:2 atomic ratio of Ni and Mn. The weakness of superlattice spots for $\text{LiNi}_{1/2}\text{Mn}_{1/2}\text{O}_2$ is well ascribed to the small order parameter due to the off-stoichiometry in the Ni/Mn atomic ratio. The lattice images corresponding to the $[\sqrt{3} \times \sqrt{3}]R30^\circ$ superlattice did not show so much difference between $\text{Li}_{2/3}\text{Ni}_{1/3}\text{Mn}_{2/3}\text{O}_2$ and $\text{LiNi}_{1/2}\text{Mn}_{1/2}\text{O}_2$.

The EDP of $\text{Li}_{2/3}\text{Ni}_{1/3}\text{Mn}_{2/3}\text{O}_2$ shows weak extra spots marked by asterisks in addition to the superlattice spots due to the $[\sqrt{3} \times \sqrt{3}]R30^\circ$ ordering. Because of the multiple twinning, the EDP is rather complex. The detailed analysis revealed that the extra spots appear at the forbidden reciprocal lattice points of Cmca lattice without any multiplicity of unit cell. The appearance of these spots indicates that the actual symmetry of $\text{Li}_{2/3}\text{Ni}_{1/3}\text{Mn}_{2/3}\text{O}_2$ is not C -centered. These spots often disappeared after the long electron beam irradiation probably because of the beam heating. The one of the possible origin of these weak extra spots may be the vacancy ordering in the Li layers. The ordering of the Li vacancies in the deintercalated LiNiO_2 and has been reported to be 2×2 type one for the compositional range of $0.5 < x < 0.75$ in Li_xNiO_2 [11]. However, no vacancy order was reported for Li_xCoO_2 . The difference in the vacancy ordered structure depending on the transition metal elements is interesting. The structural details for the Li-vacancy ordering are under investigation.

As shown in Fig. 3(b), the layer stacking of $\text{LiNi}_{1/2}\text{Mn}_{1/2}\text{O}_2$ viewed along the $[110]$ direction of rhombo-hexagonal $R\bar{3}m$ lattice is almost regular, although some twinning is observed. On the other hand, the lattice image of $\text{Li}_{2/3}\text{Ni}_{1/3}\text{Mn}_{2/3}\text{O}_2$ viewed along the $[110]$ direction of orthorhombic Cmca lattice shows many stacking faults as shown in Fig. 3(a). The corresponding EDP shows many extra spots due to the multiple twinning and also the diffuse streaks along the c^* axis. The origin of the stacking disorder is uncertain at the present stage. However, the disorder of vacancy ordering in Li layers may be one of the origins.

3.3 Thermal stability

Figure 4 shows TG profiles of $\text{Li}_{2/3}\text{Ni}_{1/3}\text{Mn}_{2/3}\text{O}_2$ and $\text{LiNi}_{1/2}\text{Mn}_{1/2}\text{O}_2$. Measurements were carried out in air stream. Heating and cooling rates were set to be $10^\circ\text{C}\cdot\text{min}^{-1}$. The temperature was held at the maximum temperature (1000°C) for 2 hours prior to the cooling. $\text{Li}_{2/3}\text{Ni}_{1/3}\text{Mn}_{2/3}\text{O}_2$ shows much larger weight change than $\text{LiNi}_{1/2}\text{Mn}_{1/2}\text{O}_2$. The TG-profile of $\text{Li}_{2/3}\text{Ni}_{1/3}\text{Mn}_{2/3}\text{O}_2$ shows the almost reversible gravimetric changes in the temperature range between 600 - 800°C . It is well assumed that the weight changes result from the oxygen release and uptake corresponding to the valence changes of transitional metals. Assuming that the nickel valence

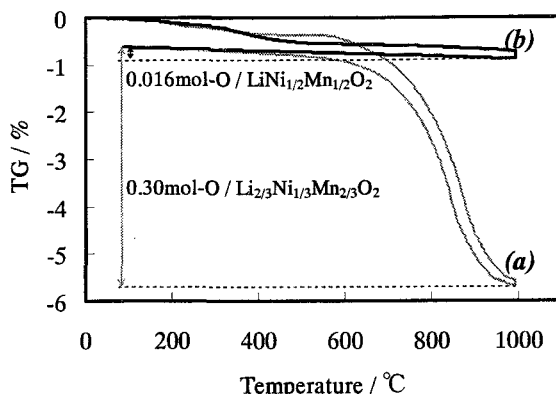


Figure 4. TG profiles of (a) $\text{Li}_{2/3}\text{Ni}_{1/3}\text{Mn}_{2/3}\text{O}_2$, and (b) $\text{LiNi}_{1/2}\text{Mn}_{1/2}\text{O}_2$

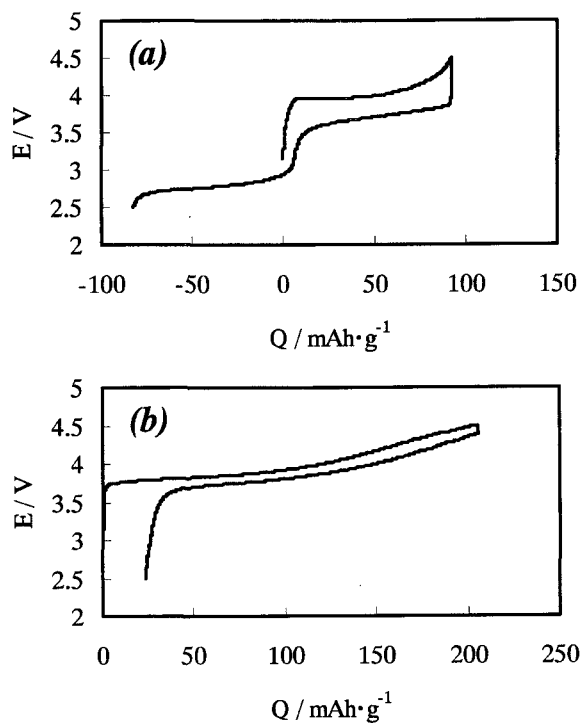


Figure 5. Charge and discharge curves of (a) $\text{Li}_{2/3}\text{Ni}_{1/3}\text{Mn}_{2/3}\text{O}_2$, and (b) $\text{LiNi}_{1/2}\text{Mn}_{1/2}\text{O}_2$.

is constant, the manganese atoms should be about trivalent at 1000°C . The smaller weight change of $\text{LiNi}_{1/2}\text{Mn}_{1/2}\text{O}_2$ means the high thermal stability and that most of the Mn atoms in tetravalent state even at 1000°C .

3.4 Electrochemical measurements

Fig. 5 shows the charge and discharge profiles of (a) $\text{Li}_{2/3}\text{Ni}_{1/3}\text{Mn}_{2/3}\text{O}_2$ and (b) $\text{LiNi}_{1/2}\text{Mn}_{1/2}\text{O}_2$. Both compounds could deliver a stable capacity of about 180mAh g^{-1} between 2.5 and 4.5V versus Li. The profile of $\text{Li}_{2/3}\text{Ni}_{1/3}\text{Mn}_{2/3}\text{O}_2$ reveals two plateaus; an upper plateau appears at around 3.9V, and a lower plateau, near 2.9V with the significant cell polarization.

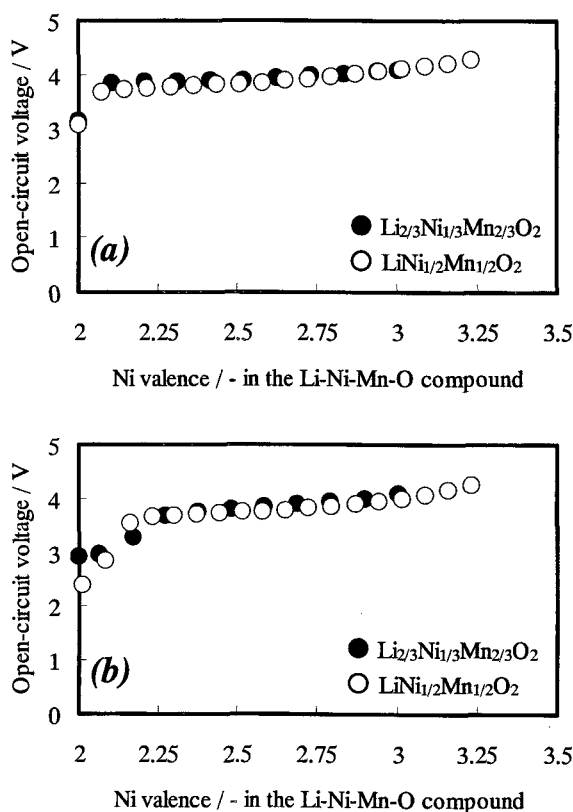


Figure 6. Open-circuit voltage (OCV) of (a) the charge state, and (b) the discharge state.

The cell polarization is ascribable to the internal resistance resulting from the structural defects as observed in Fig. 3b. J. M. Paulsen et al. [12] reported that the charging of $\text{Li}_{2/3}\text{Ni}(\text{II})_{1/3}\text{Mn}(\text{IV})_{2/3}\text{O}_2$ oxidizes Ni^{2+} to Ni^{3+} or Ni^{4+} and that the discharging will reduce Mn^{4+} to Mn^{3+} . They also reported that the initial T2 phase transforms to the O2 phase in the initial state of charging. On the other hand, $\text{LiNi}_{1/2}\text{Mn}_{1/2}\text{O}_2$ shows no plateau near 2.9V corresponding to the reduction from Mn^{4+} to Mn^{3+} . Electrochemical measurements indicate that the Mn atoms in $\text{Li}_{2/3}\text{Ni}_{1/3}\text{Mn}_{2/3}\text{O}_2$ tend to be more reducible than those in $\text{LiNi}_{1/2}\text{Mn}_{1/2}\text{O}_2$. The stability of tetravalent Mn in $\text{LiNi}_{1/2}\text{Mn}_{1/2}\text{O}_2$ is consistent with the results of thermal analysis shown in Fig. 4.

Fig. 6 shows the open-circuit voltage (OCV) plots of (a) $\text{Li}_{2/3}\text{Ni}_{1/3}\text{Mn}_{2/3}\text{O}_2$ and (b) $\text{LiNi}_{1/2}\text{Mn}_{1/2}\text{O}_2$. They were obtained from the intermittent charge and discharge measurements. The applied intermittent mode was 1h on and 12h off at a rate of 0.1mA cm^{-2} . There was no significant difference in the OCV between $\text{LiNi}_{1/2}\text{Mn}_{1/2}\text{O}_2$ and $\text{Li}_{2/3}\text{Ni}_{1/3}\text{Mn}_{2/3}\text{O}_2$. The similarity of OCV curves means that the band structures are not so different.

4. Conclusion

$\text{LiNi}_{1/2}\text{Mn}_{1/2}\text{O}_2$ and $\text{Li}_{2/3}\text{Ni}_{1/3}\text{Mn}_{2/3}\text{O}_2$ were synthesized and characterized using XRD, TEM and electrochemical measurements. Both compounds have layered rock-salt type fundamental lattices, O3 and T2 structures, respectively. Electron diffraction patterns of two com-

pounds show superlattice spots indicating $[\sqrt{3} \times \sqrt{3}]R30^\circ$ cationic ordering in the basal triangular lattice. Their intensities for $\text{LiNi}_{1/2}\text{Mn}_{1/2}\text{O}_2$ are smaller than those for $\text{Li}_{2/3}\text{Ni}_{1/3}\text{Mn}_{2/3}\text{O}_2$, probably because the off-stoichiometry. In the case of $\text{Li}_{2/3}\text{Ni}_{1/3}\text{Mn}_{2/3}\text{O}_2$, extra spots indicating a periodic compositional modulation in the Li layers were firstly observed. EDPs and TEM images of $\text{Li}_{2/3}\text{Ni}_{1/3}\text{Mn}_{2/3}\text{O}_2$ revealed many defects in the layer stacking in contrast to the almost regular stacking in the $\text{LiNi}_{1/2}\text{Mn}_{1/2}\text{O}_2$. The suppression of structural defects and the control of Ni/Mn and Li/vacancy ordering should lead to the excellent electrochemical performance of $\text{Li}_{2/3}\text{Ni}_{1/3}\text{Mn}_{2/3}\text{O}_2$. Electrochemical measurements reveal the similar OCV for both compounds, suggesting a similarity in the electronic band structure.

References

- [1] T. Ohzuku and Y. Makimura, *Chem. Lett.*, 744-745 (2001).
- [2] C. Delmas, C. Fouassier, and P. Hagenmuller, *Physica B*, **99**, 81 (1980)
- [3] J.M. Paulsen, R.A. Donabarger, and J.R. Dahn, *Chem. Mater.*, **12**, 2257-2267 (2000).
- [4] Y. Koyama, Y. Makimura, I. Tanaka, H. Adachi, and T. Ohzuku, *J. Electrochem. Soc.*, **151**, A1499-A1506 (2004)
- [5] Y.S. Meng, G. Ceder, C.P. Grey, W.-S. Yoon, and Y. Shao-Horn, *Electrochem. and Solid-State Lett.*, **7**, A155 (2004)
- [6] A. Van der Ven, G. Ceder, *Electrochem. Commun.*, **6**, 1045 (2004)
- [7] H. Kobayashi, Y. Arachi, H. Kageyama, H. Sakaebe, K. Tatsumi, S. Emura, M. Yoneyama, D. Mori, R. Kanno, T. Kamiyama, *J. Mater. Chem.*, **13**, 590-595 (2003)
- [8] J.M. Paulsen, and J.R. Dahn, *J. Electrochem. Soc.*, **147**, 2478-2485 (2000)
- [9] H. Kobayashi, Y. Arachi, H. Kageyama, H. Sakaebe, K. Tatsumi, S. Emura, M. Yoneyama, D. Mori, R. Kanno, T. Kamiyama, *J. Mater. Chem.*, **13**, 590-595 (2003)
- [10] N. Nakayama, T. Mizota, T. Ohzuku, and Y. Ueda, *Trans. Mater. Res. Soc. Jpn.*, **29**, 2559-2562 (2004)
- [11] J.P. Peres, F. Weill, and C. Delmas, *Solid State Ionics*, **116**, 19 (1999)
- [12] J.M. Paulsen, C.L. Thomas, and J.R. Dahn, *J. Electrochem. Soc.*, **147**, 861-868 (2000)

(Received December 24, 2004; Accepted April 23, 2005)